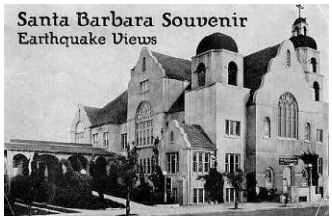

4th IASPEI / IAEE International Symposium:

Effects of Surface Geology on Seismic Motion

August 23–26, 2011 · University of California Santa Barbara

DEFINITION OF NORMALIZED ENERGY DENSITY AND ITS APPLICATION TO DIRECT ESTIMATION OF DAMPING PROPERTY

Hiroyuki Goto
Kyoto University
Uji, Kyoto, 611-0011
JAPAN

Sumio Sawada
Kyoto University
Uji, Kyoto, 611-0011
JAPAN

Yuichi Kawamura
Kyoto University
Uji, Kyoto, 611-0011
JAPAN

Toshiyuki Hirai
NEWJEC Inc.
2-3-20 Honjo-Higashi, Kita-ku,
Osaka, 531-0074
JAPAN

Takashi Akazawa
Geo-Research Institute
4-3-2 Itachibori, Nishi-ku
Osaka, 550-0012
JAPAN

ABSTRACT

We introduce a new conserved quantity, Normalized Energy Density (NED), alternative to the conventional definition of energy for a layered structure in a 2D SH problem. NED is defined by the average of power of a half transfer function multiplied by the impedance, and the conservation across the material interface is analytically proved for a two-layered case. For three, four, and ten-layered cases, the conservation is examined by applying the Monte Carlo simulation method, and then NED is supposed to be conserved through the layers. However, the conservation is not guaranteed when the material has damping. We perform another Monte Carlo simulation in order to identify the effect on NED of the damping property by applying the conventional Haskell matrix method with the damping coefficient and the apparent quality factor Q_a. NED decreases as the damping coefficient increases, and also almost the same characteristics are obtained by the apparent quality factor. The magnitude of damping properties corresponds to the decreases of NED observed in the top layer, whereas the NEDs vary widely. We introduce another damping property, T/Q, considering a travel time from the basement to the free surface, and its variation becomes smaller. We also propose the analytical relation of NED v.s. T/Q to give almost the upper boundary of the possible solution. The correlation curve enables us to identify the damping property directly from NED.

INTRODUCTION

Conserved quantities, such as mass, momentum and energy, in elasto-dynamic problems are the fundamental variables when analyzing wave propagation in a continuous medium. In addition, the balance principles associated with these quantities, e.g., the balance of mass and the balance of momentum, govern the deformation within the framework of Newtonian mechanics. The balance of energy is one of the principles used to quantify the seismic energy radiated from an earthquake source.

Radiation energy E is theoretically defined as the total energy transmitted through a certain surface. When a particular region, e.g. a seismic fault, generates all of the energy, the integration on the arbitrary surface surrounding the region is theoretically conserved even for a general heterogeneous medium. The representation has already been introduced in Love (1927). The energy of seismic events was first applied by Richter (1935) in order to measure the size of earthquakes by using the local magnitude scale, although it was not exactly equal to the definition of the energy. Afterward, Kanamori (1977) proposed the use of moment magnitude, defined from the seismic moment that is related to the energy release during the events, whose energy is different from the radiation energy. A detailed discussion on radiation energy is introduced in Kostrov and Das (1988), Fukuyama (2005), and Abercrombie *et al.* (2006).

If a seismic wave through the surface S is approximated by a single plane wave, either a P- or an S-wave propagated in a uniform direction, the energies are represented as $E_P = \int_0^\infty dt \int_S \rho\alpha \dot{Y}_\alpha^2 l_i n_i dS$ and $E_S = \int_0^\infty dt \int_S \rho\beta \dot{Y}_\beta^2 l_i n_i dS$, where ρ, α and β are the density, the P-wave velocity, and the S-wave velocity, respectively. $\dot{Y}_\alpha$ and $\dot{Y}_\beta$ are the amplitudes of particle velocity for the P-wave and the S-wave, respectively. l_i is a vector representing the direction of the wave propagation. The energy density, defined by the integrand, is a product of the square of the particle velocity and the impedance.

A part of the energy integrated on the shrunken area of S is utilized as a principle of energy conservation when all of the input energy is confined in a certain region, so-called "ray tube" (Aki and Richards, 2002). The energy on the cross-sectional area of the tube is theoretically conserved. Here, we focus on the layered structure. At the interface, part of the energy for the input wave is transmitted, and the rest is reflected. Then, both the transmitted and the reflected waves should be considered in order to apply the energy conservation in the ray tube. The sum of the transmitted energy and the reflected energy is equal to the input energy. However, the total input energy can not be observed in only the opposite layer because the transmitted energy is part of the input energy. Therefore, the energy is not conserved across the interfaces. Note that some researchers apply the energy, directly defined by $\int_0^\infty \rho c \dot{Y}^2 dt$, to the layered structure (e.g., Kokusho and Motoyama, 2002), however, they do not pay attention to the fact that the quantity is not conserved. If a quantity conserved over the layer structure exists, absorbed energy in propagating in the layer might be estimated, directly. The quantification of the absorbed energy helps to understand the hysteretic damping due to anelasticity, e.g. Q-factor, and the soil nonlinearity, as discussed in Kokusho and Motoyama (2002).

Goto *et al.* (2011) proposes alternative quantity, Normalized Energy Density (NED), for the elastic layered structure. NED has a utilitarian characteristic that it is conserved through the layers. In this article, we introduce NED and its application to the direct estimation of the damping property.

NORMALIZED ENERGY DENSITY (Goto *et al.*, 2011)

Two-layered case

The theoretical implementation starts from the waves, vertically propagated into a simple two-layered structure. Only 2D SH waves, which have an antiplane amplitude with respect to the plane, are considered here. The structure consists of a horizontal layer, Layer #1, with a thickness of h and a half space basement, Basement #0. The S-wave velocity and the density are β_1 and ρ_1 for Layer #1 and β_0 and ρ_0 for Basement #0, as shown in Fig. 1. An incident plane wave propagates vertically into Layer #1 through the interface between Layer #1 and Basement #0. Each layer keeps elasticity independent of the wave amplitude.

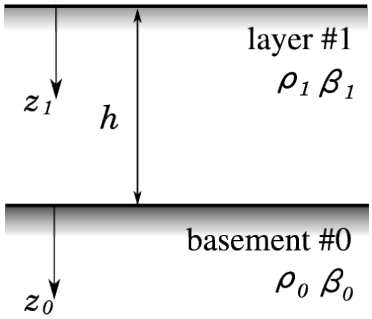

Fig. 1. Two-layered model.

We define real functions P_1 and P_0 as the square of the absolute value of the upgoing wave amplitudes A_1 and A_0 normalized by input wave amplitude.

$$P_1(\omega) \equiv \left| \frac{A_1(\omega)}{A_0(\omega)} \right|^2 = \frac{1}{\cos^2(\omega h/\beta_1) + R_{1,0}{}^2 \sin^2(\omega h/\beta_1)} \tag{1}$$

$$P_0(\omega) \equiv \left| \frac{A_0(\omega)}{A_0(\omega)} \right|^2 = 1 \tag{2}$$

where $R_{1,0}$ represents an impedance ratio ($=\rho_1\beta_1/\rho_0\beta_0$). P_1 is a single-valued function with respect to $\cos(\omega h/\beta_1)$, and a periodic function of $\omega h/\beta_1 = n\pi$ ($n \in \boldsymbol{N}$). Moreover, P_1, defined in $\omega h/\beta_1 \in [0,\pi]$, is symmetric about $\pi/2$. Therefore, the average of P_1 in

$\omega \in [-\infty, \infty]$, defined by $\langle P_1 \rangle$, is equal to the average of P_1 in $\omega h/\beta_1 \in [0, \pi/2]$.

$$\begin{aligned} \langle P_1 \rangle &= \lim_{\Omega \to \infty} \frac{1}{\Omega} \int_{-\Omega/2}^{\Omega/2} \frac{1}{\cos^2(\omega h/\beta_1) + {R_{1,0}}^2 \sin^2(\omega h/\beta_1)} d\omega \\ &= \frac{2}{\pi} \int_0^{\pi/2} \frac{d\tilde{\omega}}{\cos^2(\tilde{\omega}) + {R_{1,0}}^2 \sin^2(\tilde{\omega})_0} = \frac{2}{\pi} \cdot \frac{\pi}{2R_{1,0}} = \frac{1}{R_{1,0}} \end{aligned} \tag{3}$$

Thus, the average of P_1 is equal to the inverse of impedance ratio $R_{1,0}$. When the input wave satisfies $|A_0(\omega)| = 1$, $\langle P_1 \rangle$ represents the average power for the upgoing waves in Layer #1 or for half the amplitude of the waves observed on the free surface. On the other hand, the average of P_0 is identical to 1 because of P_0=1.

$$\langle P_0 \rangle = 1 \tag{4}$$

We define a quantity, a product of the average of P and the impedance $\rho\beta$, such as $\rho_1\beta_1\langle P_1 \rangle$ for Layer #1 and $\rho_0\beta_0\langle P_0 \rangle$ for Basement #0. From the explicit representations of $\langle P_1 \rangle$ and $\langle P_0 \rangle$ by Eqs.(3)-(4), the following relation is obtained:

$$\rho_1\beta_1\langle P_1 \rangle = \rho_0\beta_0\langle P_0 \rangle \tag{5}$$

Equation (5) includes some physical features. Both the left- and right-hand sides are the average power of the upgoing waves multiplied by the impedance at each layer. This means that the quantity, $\rho\beta\langle P \rangle$, is conserved across the interface. Moreover, the quantity is directly evaluated from the transfer function. We name the quantity $\rho\beta\langle P \rangle$, Normalized Energy Density (NED).

Multi-layered case

We consider a multi-layered structure consisting of n layers (#1-#n) over Basement #0, as shown in Fig. 2. The S-wave velocity of Layer #k is β_k, the density is ρ_k, and the thickness is h_k. 2D SH waves vertically propagate vertically into the layers through the interface between Layer #n and Basement #0.

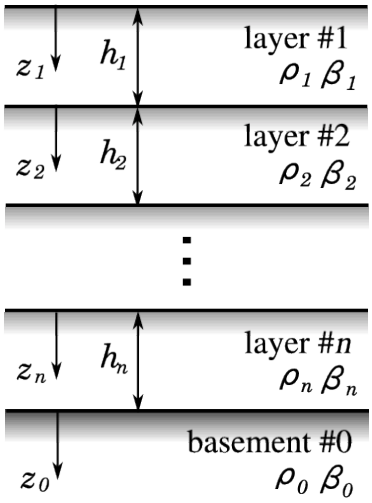

Fig. 2. Multi-layered model.

From the boundary conditions at the interface between Layers #(k+1) and #k, the amplitudes for Layer #(k+1) are represented by those for Layer #k as

$$\begin{pmatrix} A_{k+1} \\ B_{k+1} \end{pmatrix} = \begin{bmatrix} \frac{1}{2}(1+R_{k,k+1})\alpha_k & \frac{1}{2}(1-R_{k,k+1})\alpha_k^* \\ \frac{1}{2}(1-R_{k,k+1})\alpha_k & \frac{1}{2}(1+R_{k,k+1})\alpha_k^* \end{bmatrix} \begin{pmatrix} A_k \\ B_k \end{pmatrix} \tag{6}$$

where A_k and A_{k+1} are the amplitudes for the upgoing waves, and B_k and B_{k+1} are those for the downgoing waves. $R_{k,l}$ is the impedance ratio ($= \rho_k\beta_k/\rho_l\beta_l$). α_k represents the complex variables defined by $\alpha_k = e^{i\omega h_k/\beta_k}$. Hereinafter, each component of the matrix in Equation (6) is indicated by $T_{ij}^{\,k}$ as

$$\begin{bmatrix} T_{11}^k & T_{12}^k \\ T_{21}^k & T_{22}^k \end{bmatrix} = \begin{bmatrix} \frac{1}{2}(1+R_{k,k+1})\alpha_k & \frac{1}{2}(1-R_{k,k+1})\alpha_k^* \\ \frac{1}{2}(1-R_{k,k+1})\alpha_k & \frac{1}{2}(1+R_{k,k+1})\alpha_k^* \end{bmatrix} \tag{7}$$

The amplitudes for Layer #k are represented by those for Layer #1 by applying Equation (6), recursively, and the traction-free condition on the free surface, $A_1 = B_1$, gives the following representation of the amplitudes:

$$\begin{cases} A_k = C_{k-1} A_1 \\ A_0 = C_n A_1 \end{cases} \tag{8}$$

where C_k is defined as follows:

$$C_k = T_{1i}^{k} \cdot T_{ij}^{k+} \cdots T_{lm}^{2} \cdot \left(T_{m1}^{1} + T_{m2}^{1} \right) \tag{9}$$

We also define NED by $\rho\beta\langle P \rangle$, and the explicit representation is given as follows:

$$\begin{aligned} \rho_k \beta_k \langle P_k \rangle &\equiv \lim_{\Omega \to \infty} \frac{1}{\Omega} \int_{-\Omega/2}^{\Omega/2} \rho_k \beta_k \left| \frac{A_k(\omega)}{A_0(\omega)} \right|^2 d\omega \\ &= \lim_{\Omega \to \infty} \frac{1}{\Omega} \int_{-\Omega/2}^{\Omega/2} \rho_k \beta_k \frac{\left(\Re[\alpha_{k-1} C_{k-2}] \right)^2 + R_{k-1,k}^{\ 2} \left(\Im[\alpha_{k-1} C_{k-2}] \right)^2}{\left(\Re[\alpha_n C_{n-1}] \right)^2 + R_{n,0}^{\ 2} \left(\Im[\alpha_n C_{n-1}] \right)^2} d\omega \end{aligned} \tag{10}$$

If the integration results becomes $1/R_{k,0}$, NED is conserved through all the layers. Therefore, we apply the Monte Carlo simulation method in order to examine the conservation of NED for the cases with more than three layers.

For the three- and the four-layered cases, five hundred sets of physical values are also generated from random numbers within the range of 10-700 m/s for the S-wave velocity and 1000-2000 kg/m^3 for the density of every layer and for Basement #0. The total thickness of the layers is generated within the range of 1-50 m and then divided into layers with a random thickness.

Figure 3 shows three samples of P_1 normalized by $1/R_{1,0}$ for the three-layered and four-layered cases. P_1 are almost distributed around 1. NED between the layers is checked in Figs. 4-5. The integrations are also approximated by the numerical integration every 1.0 s^{-1} within 1.0-2.5e5 s^{-1}. Every sample is on the reference line, and thus, NED is expected to be conserved through the layers even for the three- and the four-layered cases.

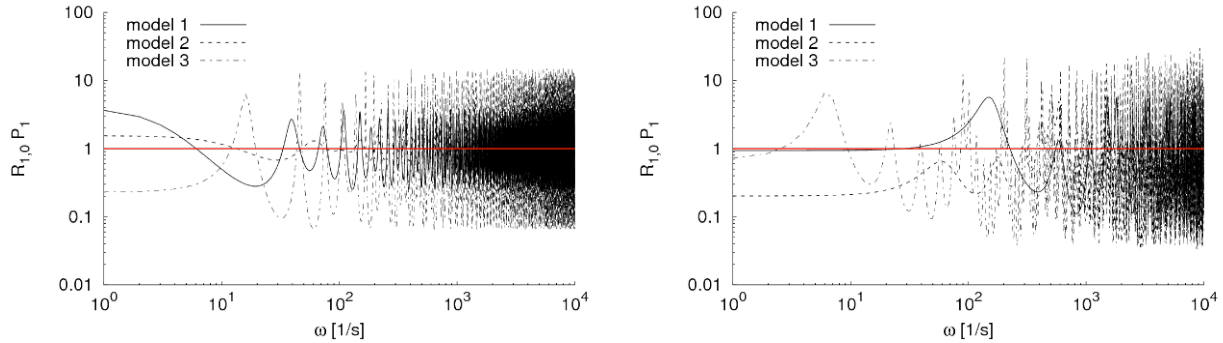

Fig. 3. Samples of P1 normalized by 1/ for the three-layered case (left) and the four layered case (right)

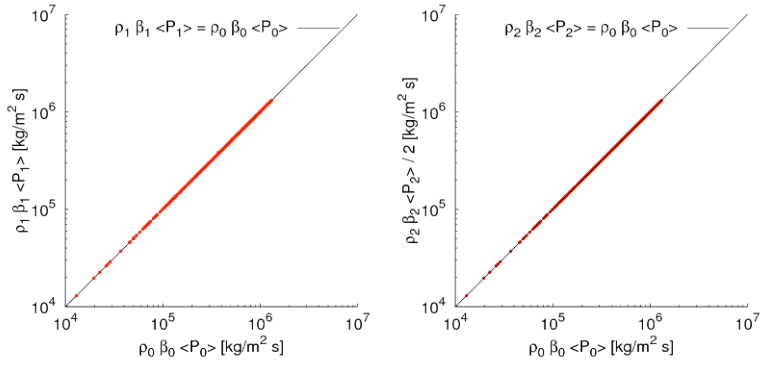

Fig. 4. Comparison of NED between Layer #1 and Basement #0 (left) and between Layer #2 and Basement #0 (right) for the three-layered case.

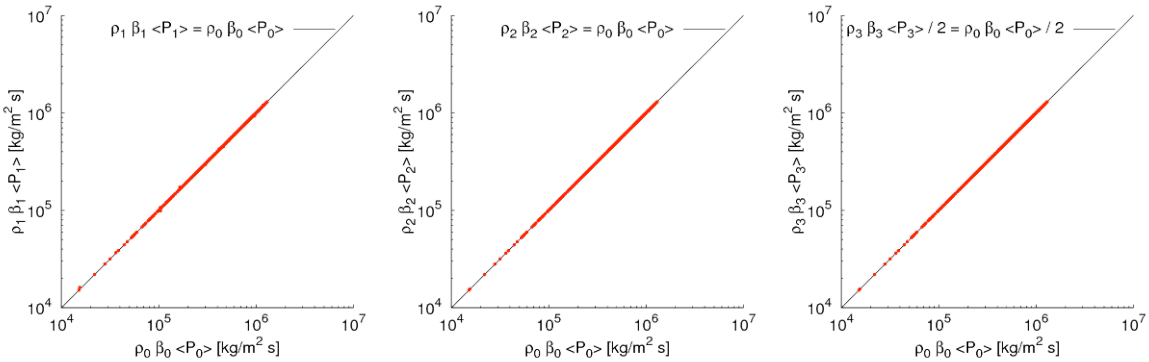

Fig. 5. Comparison of NED between Layer #1 and Basement #0 (left), between Layer #2 and Basement #0 (middle), and between Layer #3 and Basement #0 (right) for the four-layered case.

The simulations are applied to a ten-layered case. Five hundred sets of physical values are generated from the random numbers within the range of 10-700 m/s for the S-wave velocity and 1000-2000 kg/m^3 for the density of every layer and for Basement #0. The total thickness of the layers is generated within the range of 1-50 m, and then divided into layers with a random thickness. NED at Layer #1 and Basement #0 is compared in Fig. 6. The integrations are approximated by a numerical integration every 0.02 s^{-1} within 0.02-1.6e7 s^{-1}. Almost all the samples are on the reference line, and thus, NED is expected to be conserved between Layer #1 and Basement #0. The depth distribution of NED normalized by that of the basement is also shown in Fig. 6. The quantities are almost constant at 1 for all the layers. Therefore, the results of the Monte Carlo simulation support the conservation of NED through the layers.

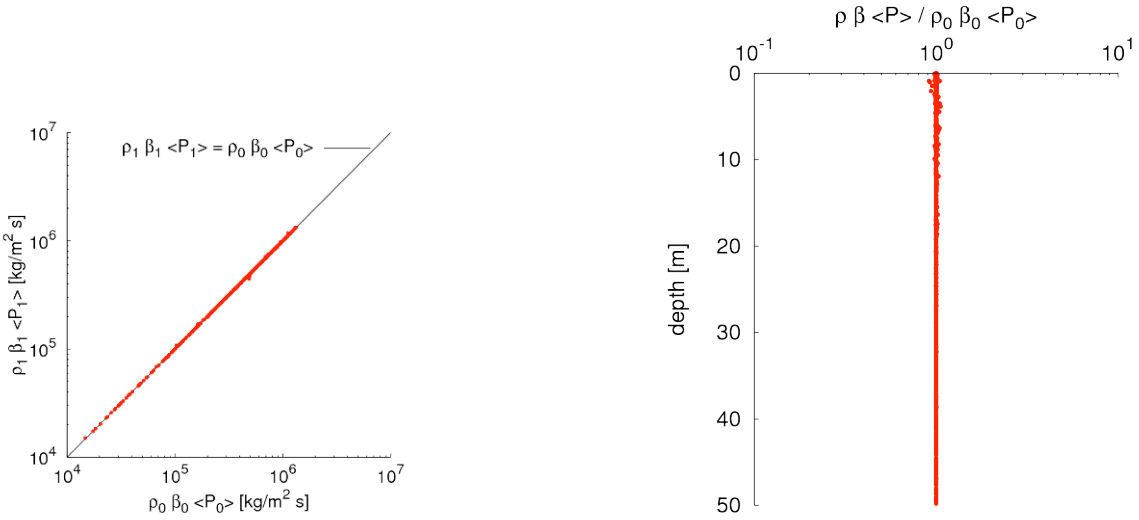

Fig. 6. Comparison of NED for the ten-layered case between Layer #1 and Basement #0 (left), and depth distribution of NED normalized by NED at Basement #0 (right)

EFFECT OF INTERNAL DAMPING

In order to account for the effect of internal damping on NED, we introduce two different types of representation, a complex stiffness and an apparent quality factor. The complex stiffness is a conventional way to introduce the internal damping to the waves propagating in a layered structure. The representation of the stiffness is, as follows:

$$\mu^* = \mu(1 + 2ih) \tag{11}$$

where μ is the shear stiffness defined by $\rho\beta^2$. h is the damping coefficient. i is an imaginary unit. The damping coefficient h is introduced by applying the complex representation to Haskell matrix method (Haskell, 1960).

On the other hand, internal damping of the crust structure is also represented by a quality factor Q. The definition of Q is the decay of the energy in propagating wave.

$$Q = 2\pi \frac{E}{\Delta E} \tag{12}$$

where E is an excitation energy per a cycle, and ΔE is a decreasing of energy per a cycle. For the waves propagating in the homogeneous material, Q is related with the damping coefficient as $Q = 1/2h$. In the case, the decay of plane wave amplitude in a distance of x, $A(x)/A(0)$, is analytically represented as,

$$\frac{A(x)}{A(0)} = \exp\left(\frac{-\omega x}{2\beta Q}\right) \tag{13}$$

where x is the traveled distance of wave. However, if the above representation is directly applied to the layered structure, the quality factor in Equation (13) is not equal to $1/2h$. For the layered structure, we apply another definition similar to the quality factor, an apparent quality factor Q_a, to the response $A_k(z_k)$ at the depth of z_k in Layer #k as,

$$A_k(z_k) = A_k^{\text{no damping}} \exp\left(\frac{-\omega T(z_k)}{2Q_a}\right) \tag{13}$$

where $A_k^{\text{no damping}}$ is the response calculated from Haskell matrix method without the internal damping. $T(z_k)$ is the travel time of shear wave from the basement to the depth z_k. The apparent quality factor Q_a is not guaranteed to be equal to $1/2h$.

The effect of the damping coefficient h and the apparent quality factor Q_a is examined by applying Monte Carlo simulations for two- and six-layered cases. Three thousand sets of physical values are generated from random numbers within the range of 50-1000 m/s for the S-wave velocity and 1400-2400 kg/m^3 for the density of every layer and the basement. The total thickness of the layers is generated within the range of 100-1000 m. The thickness is divided into layers with a random thickness, and the layers are sorted by ascending order of the layer thickness from the top of the layer.

For each sample, 4 types of the damping coefficients, h=0, 0.005, 0.02, and 0.05 are simulated, and the corresponding apparent quality factor Q_a=100, 25, and 10 are also simulated. For six-layered case, the damping coefficients are assumed to be constant through the layers, while no internal damping is considered in the basement. The integrand of the original definition of NED is averaged from the negative infinite to the positive infinite, whereas the definition is not applicable to the simulation results because the high frequency component is vanished due to the internal damping. Then, we truncated the high frequency component by taking the average within 0.1-20 Hz.

Figure 7 and 8 show the effect of the internal damping on NED for two- and six-layered cases, respectively. The horizontal axis is the ratio of NEDs on the free surface NED_1 and the basement NED_0. The vertical axis is the number of samples. As increasing the internal damping, the ratio of NEDs decreases, and the variation increases. The differences of the distributions calculated from the damping coefficient and the apparent quality factor are not significant for two-layered case, whereas the differences are recognized for six-layered case.

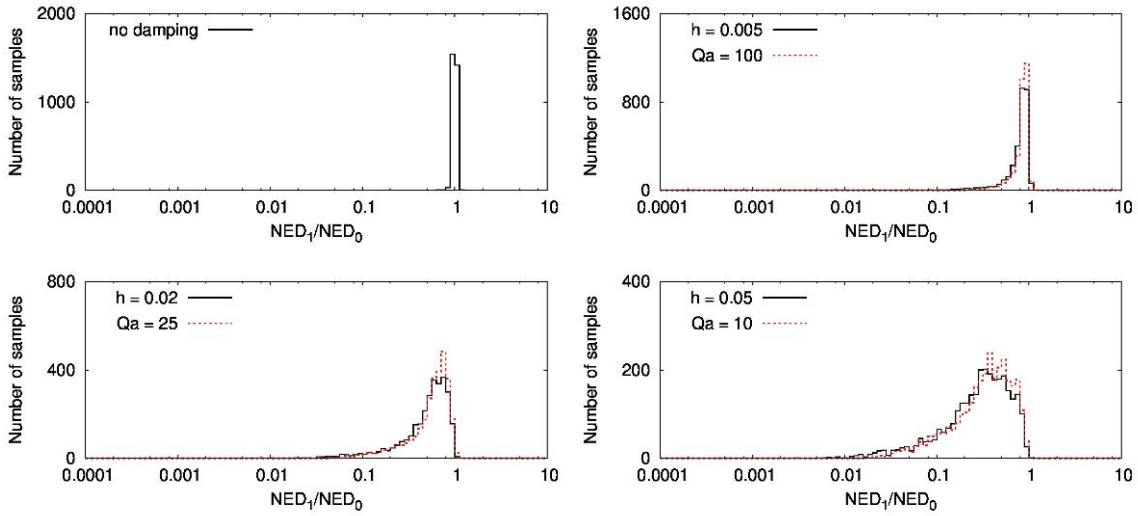

Fig. 7. Comparison of the effect of internal damping calculated by the damping coefficient and the apparent quality factor for two-layered case.

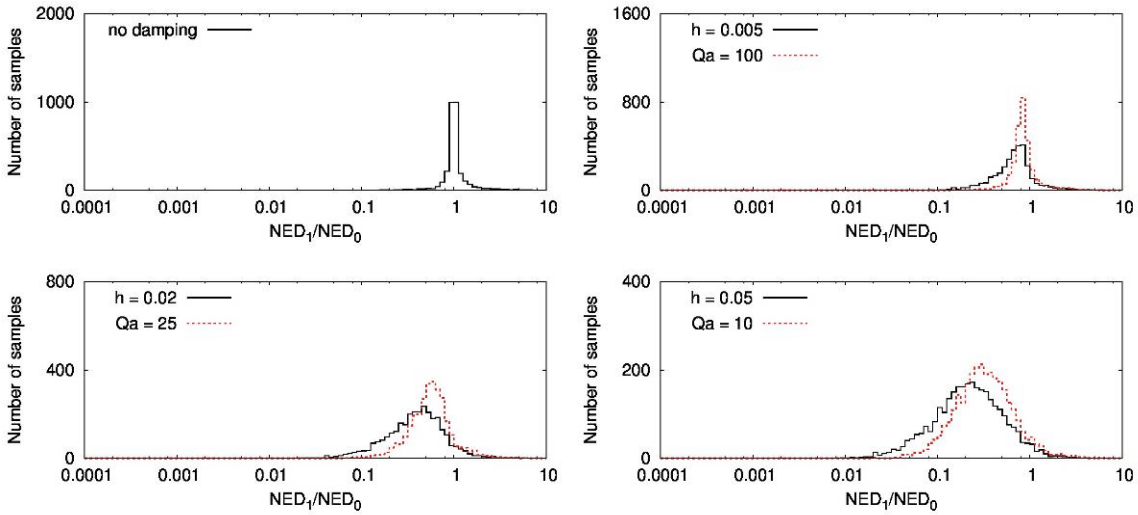

Fig. 8. Comparison of the effect of internal damping calculated by the damping coefficient and the apparent quality factor for six-layered case.

Both the damping coefficient and the apparent quality factor give too broad distribution of the ratio of NEDs to directly identify the internal damping from it. That is because the travel time T from the basement to the free surface is also the parameter controlling the responses on the free surface, as seen in Equation (13). Here, we introduce T/Q to quantify the internal damping of the layered structure, defined by the summation of physical parameters in each layer.

$$T/Q = \sum_{k=1}^{n} \frac{2H_k h_k}{\beta_k} \tag{14}$$

Figure 9 shows the comparison between the ratio of NEDs and T/Q for two- and six-layered cases. The horizontal axis is T/Q, and the vertical axis is the ratio of NEDs. The plots indicate the simulation results calculated by every damping coefficient, h=0, 0.005, 0.02, and 0.05. The ratio of NEDs is clearly correlated with T/Q regardless of the values of the damping coefficient. The correlation for six-layered case is less than that for two-layered case, whereas the correlation curve is almost similar in both cases.

We also show another simulation result for the six-layered case with a variable damping coefficient for each layer instead of the uniform values. Ten thousand sets of physical values are generated from random numbers within the same range as the previous simulations, while the damping coefficient h is also generated from random numbers within 0-0.05. Figure 10 shows the comparison between the ratio of NEDs and T/Q. This also indicates the correlation between them.

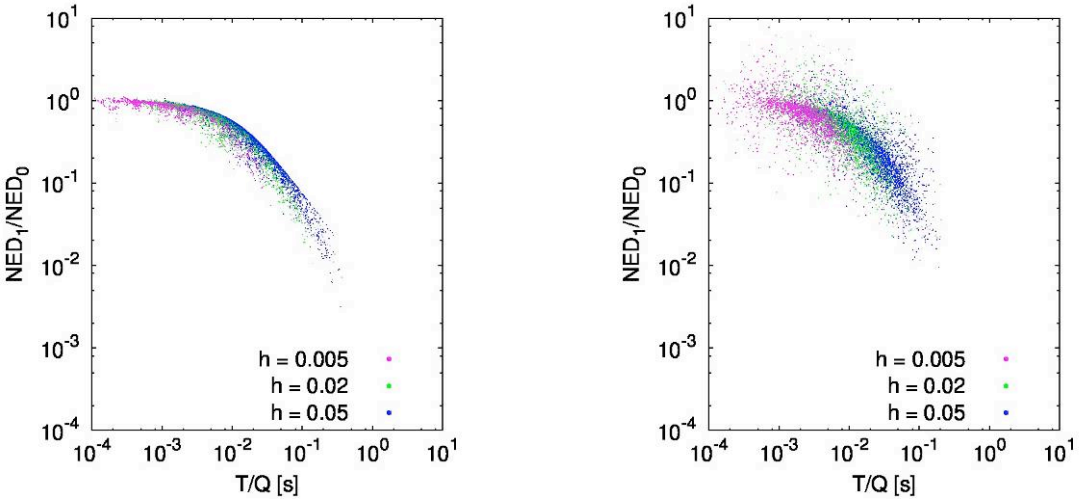

Fig.9. Comparison of the effect of T/Q for two-layered case (left) and six-layered case (right).

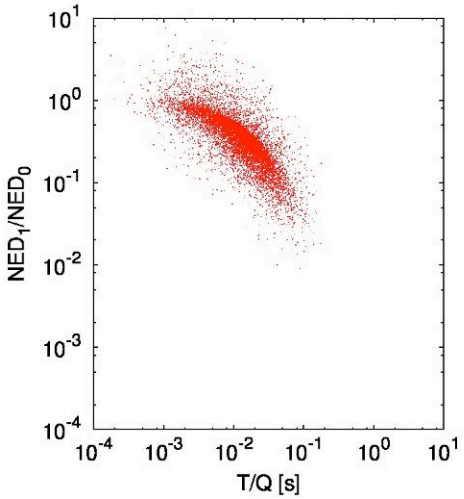

Fig.10. Comparison of the effect of T/Q for six-layered case with a variable damping coefficient.

We focus on one of the typical cases, the same physical parameters between the layers and the basement. It is actually a homogeneous half space case, whereas it belongs to the group generated by the Monte Carlo simulations. If the response for the typical case is calculated by the apparent quality factor Q_a via Equation (13), the ratio of NEDs is analytically derived as,

$$\frac{\mathrm{NED}_1}{\mathrm{NED}_0} = \frac{1}{39.8\pi}\int_{0.2\pi}^{40\pi} \exp\left(\frac{-\omega T}{Q_a}\right) d\omega \equiv F(T/Q_a) \tag{15}$$

As shown in Equation (14), the definition of T/Q is not actually equal to T/Q_a. However, we plot the line of the function $F(T/Q)$ on Figs.9 and 10, and show in Figure 11. For two-layered case, the line is almost located on the upper boundary of the samples. For both six-layered cases, the line almost lies on the upper side of the main cluster. This indicates the correlation of the ratio of NEDs and T/Q helps to estimate the internal damping from NED directly, and the analytical representation by Equation (15) gives information of almost the upper boundary of the possible solutions.

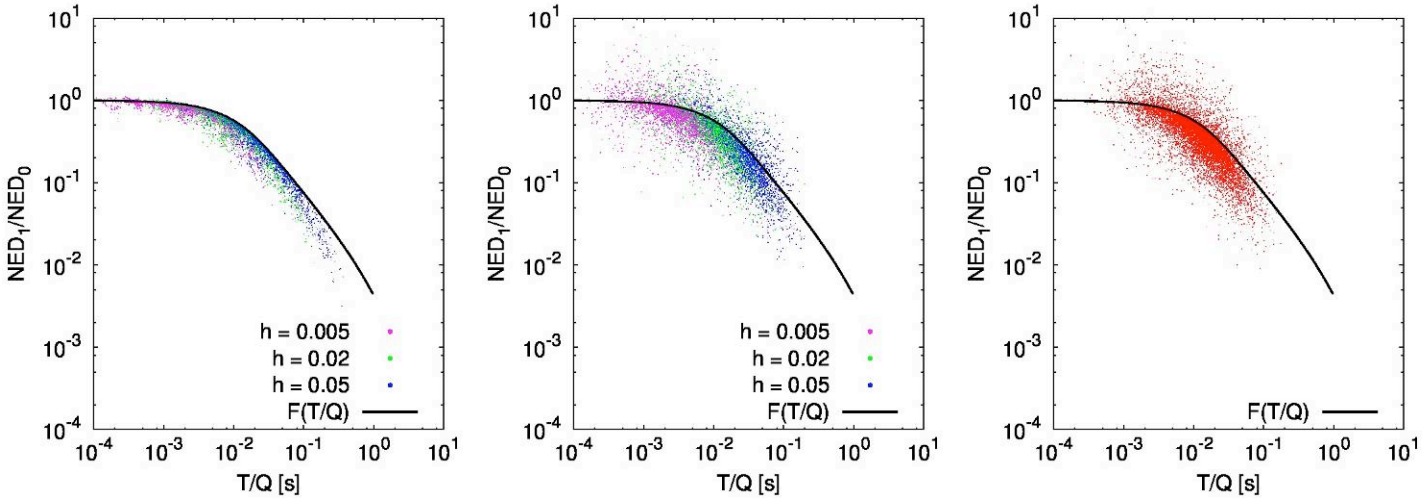

Fig. 11. Comparison of the analytical function F(T/Q) and the results for two-layered case (left), six-layered case with a uniform damping coefficient (middle), and six-layered case with a variable damping coefficient (right).

ESTIMATION OF T/Q AT KATAGIHARA AREA

Katagihara area at Kyoto Prefecture Japan caught a local damage during 1995 Kobe earthquake even about 70 km away from the epicenter (e.g., Akamatsu *et al.*, 1997). The elevation of the area is about 40 m. On the other hand, Katsura campus of Kyoto University is only 1 km away from the area, while the elevation rapidly increases to 150 m. The locations of Katagihara area and Katsura campus are shown in Figure 12. Stations observing strong ground motions are settled in both the areas, namely KTR station in Katsura campus and KTG station in Katagihara area. The stations are managed by the Committee of Earthquake Observation and

Research in the Kansai Area (CEORKA) since 1996 for KTG, and since 2009 for KTR stations.

Figure 12 also shows the borehole data and SPT N values in about 20 m of depth. Rock layer appears at the depth of 6 m at KTR, while sand and gravel layers continue to the depth of 20 m at KTG. About 10 of N value are observed around the depth of 15 m at KTG. This indicates KTG is located on softer soil ground than KTR, and KTR is almost located on the rock. Here, we assume KTR is settled on the bedrock, and the bedrock is the basement beneath KTG station. Under the assumption, the input motions through the basement to KTG are evaluated from the observation at KTR. Then, the amplification of the layers $|A_1 / A_0|$ is directly calculated from the observed data of KTR and KTG.

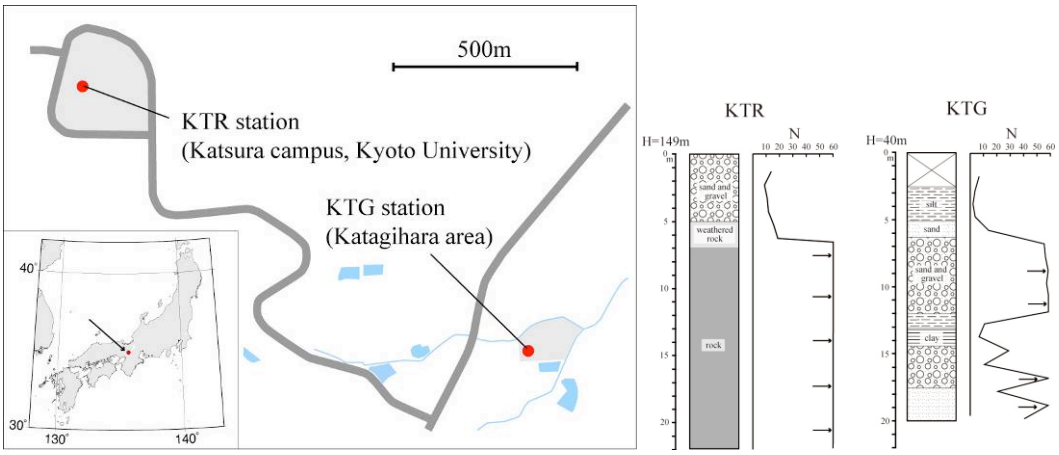

Fig.12. Location of KTR and KTG stations and the borehole data.

Local earthquakes within 150 km of the epicenter distance and observing ground motions at both KTR and KTG stations are selected until the end of 2010. Figure 13 shows the epicenter locations of selected 9 earthquakes. The hypocenters depth of eight events located close to the stations (#1-#7 and #9) are about 10 km, and the other (#8) is 60 km. The spectrum ratios KTG/KTR are calculated by dividing the Fourier spectrum of KTG by KTR for each horizontal component, which are smoothed by a 0.1 Hz width of window. The average spectrum ratio is evaluated by averaging over all events and the components. Figure 13 also shows the spectrum ratios KTG/KTR of each event and the average spectrum ratio. The peaks of the spectrum ratio KTG/KTR are recognized at around 0.5 Hz, 2 Hz, and 6 Hz.

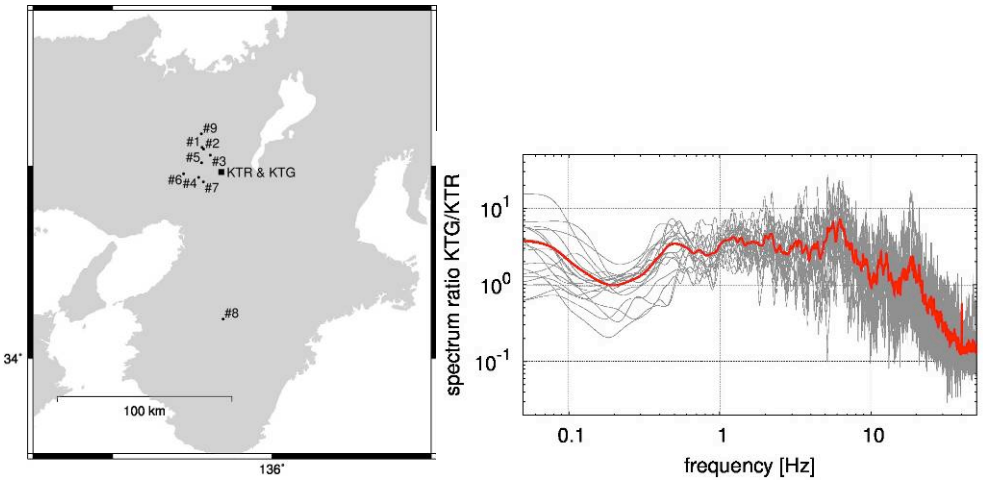

Fig.13. Location of epicenter for selected 9 earthquakes (left) and the spectrum ratio of KTG/KTR (right).

Conventional method to estimate the internal damping of layered structure is to evaluate appropriate velocity, density and damping coefficient models, and fit the synthetic spectrum ratio to the observed one. After the iterative procedures, the internal damping is estimated as the damping coefficient model. First, we try to estimate the internal damping by the conventional method. The initial models of S-wave velocity and density consist of five layers and the basement, and the values are manually estimated to represent the average spectrum ratio KTG/KTR. And then, the more appropriate values are searched by applying simple Genetic Algorithm (GA) with a population of 100, a generation of 200, a mutation probability of 0.5%, and a crossover probability of 75%. The search ranges of each parameter are set within 80-120% of the initial values. Table 1 shows the final model of the layered structure beneath KTG,

and Figure 14 shows the comparison of the synthetic spectrum ratio KTG/KTR to the observed average spectrum ratio. The model well represents the peak frequencies and the values of the observation.

Tbl.1. Final model of layered structure beneath KTG.

Layer	Top depth [m]	S-wave velocity [m/s]	Damping coefficient
#1	0	94.4	0.065
#2	4.0	235.6	0.034
#3	11.1	210.7	0.058
#4	16.4	293.8	0.028
#5	54.0	777.8	0.012
#0	379.1	1919.5	0.0

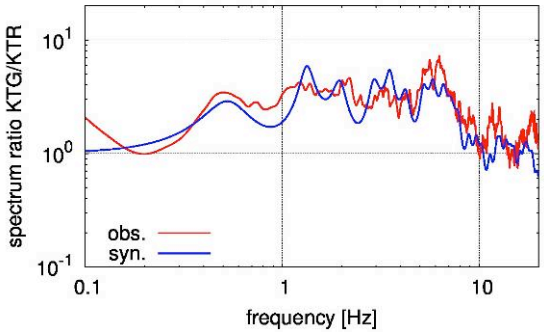

Fig.14. Comparison of the spectrum ratio KTG/KTR to the synthetic result from the final model.

On the other hand, we estimate the internal damping directly from the ratio of NEDs by applying the correlation curve explained in the previous chapter. The impedances are required in calculating NEDs on the basement and the free surface, which correspond to the impedances of the top layers at KTR and KTG, respectively. The variables may be estimated by using a simple geophysical exploration only on the free surface, whereas they are not available at this time, unfortunately. In this analysis, the final model of the impedances for the basement and the top layer are applied to calculate NED. NED on the free surface, NED_1, is evaluated by integrating the power of the averaged spectrum ratio KTG/KTR within 0.1-20 Hz, and the value is calculated as 1006146 kg/sm^2. NED on the basement #0, NED_0, is 4606919 kg/sm^2. Thus, the ratio of NEDs is calculated as 0.218.

Ten thousand sets of physical values are generated from random numbers within the same range as the previous simulations in Figure 10. However, the impedances of the top layer and the basement are constrained to the values of final model in Table 1. Figure 15 shows the comparison of the ratio of NEDs and T/Q. The calculated NED ratio 0.218 is also denoted in the plot. The right figure of Figure 15 shows the histogram of T/Q corresponding to the ratio of NEDs in 0.15-0.25. The possible values of T/Q are distributed in the range of 0.005-0.03 s. From the conventional method, T/Q = 0.0277 is calculated from the final model, and the value is consistent with the distribution in Figure 15.

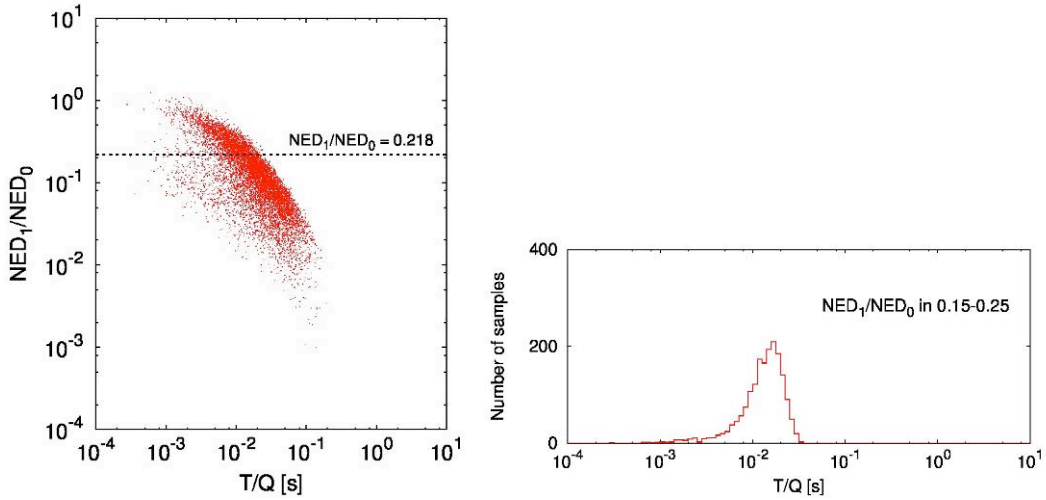

Fig.15. Monte Carlo simulation results and histogram of T/Q corresponding to the range in 0.15-0.25 of the ratio of NEDs.

CONCLUSION

We propose Normalized Energy Density for the layered structure. NED is defined by the average of power of a half transfer function multiplied by the impedance, and the conservation across the material interface is analytically proved for a two-layered case. For three, four, and ten-layered cases, the conservation is examined by applying the Monte Carlo simulation method, and then NED is

supposed to be conserved through the layers. We perform another Monte Carlo simulation in order to identify the effect on NED of the damping property by applying the conventional Haskell matrix method with the damping coefficient and the apparent quality factor Q_a. NED decreases as the damping coefficient increases, and also almost the same characteristics are obtained by the apparent quality factor. The magnitude of damping properties corresponds to the decreases of NED observed in the top layer, whereas the NEDs vary widely. We introduce another damping property, T/Q, considering a travel time from the basement to the free surface, and its variation becomes smaller. We also propose the analytical relation of NED v.s. T/Q to give almost the upper boundary of the possible solution. The correlation curve enables us to identify the damping property directly from NED.

We estimated the damping property of T/Q at Katagihara area by applying the relation of the ratio of NEDs and T/Q, directly. The value is about 0.005-0.03 s. On the other hand, we estimated the damping coefficients by the conventional method, and T/Q is estimated as 0.0277 consistent with the proposed method. Notice that the proposed method does not require the inversion procedure and data fitting. However, we need to create a technique to directly identify the impedance on the free surface in order to calculate NED.

REFERENCES

Abercrombie, R.A., McGarr, G. Toro, and H. Kanamori [2006], "Earthquakes: radiated energy and the physics of faulting", American Geophysical Union, Washington, DC.

Akamatsu, J., Nishimura, K., Morikawa, H., Sawada, S., Onoue, K., Saito, H., Jido, M., Kagawa, T., Kamura, K. Sato, K., Furuno, K., and Masai Komazawa [1997], "Chapter 13 Bedrock structure around faults and its relation to earthquake disaster", Developments in Geotechnical Engineering, Vol.81, pp.199-216.

Aki, K. and P. G. Richards [2002], "*Quantitativ Seismology 2nd edn*", University Science Books, California.

Fukuyama, E. [2005], "Radiation energy estimated at earthquake source", Geophys. Res. Lett. Vol. 32, L13308.

Goto, H., S. Sawada and T. Hirai [2011], "Conserved quantity of elastic waves in multi-layered media: 2D SH case -Normalized Energy Density-", Wave Motion, in printing.

Haskell, N.A. [1960], "Crustal reflection of plane SH waves", J. Geophys. Res. Vol.65, pp.4147-4151.

Iwata, T. and K. Irikura [1988], "Source parameters of the 1983 Japan sea earthquake sequence", J. Phys. Earth. Vol. 36, pp.155–184.

Kanamori, H. [1977], "The energy release in great earthquakes", J. Geophys. Res. Vol. 82, pp.2981–2987.

Kinoshita, S. [1994], "Frequency-dependent attenuation of shear waves in the crust of the southern Kanto area, Japan", Bull. Seism. Soc. Am. Vol. 84, pp.1387–1396.

Kokusho, T. and R. Motoyama [2002], "Energy dissipation in surface layer due to vertically propagating SH wave", J. Geotech. Geoenv. Eng. Vol.128, pp.309–318.

Kostrov, B.V. and S. Das [1988], "*Principles of earthquake source mechanics*", Cambridge University Press, Cambridge, 1988.

Love, A.E.H. [1927], "*A treatise on the mathematical theory of elasticity*", Dover Pubns, New York.

Richter, C. [1935], "An instrumental earthquake magnitude scale", Bull. Seism. Soc. Am. Vol. 25, pp.1–32.

Sato, T. [1985], "Rupture characteristics of the 1983 Nihonkai-chubu (Japan sea) earthquake as inferred from strong motion accelerograms", J. Phys. Earth. Vol. 33, pp.525–557.